Mass Transfer from a Solid Soluble Sphere to a Flowing Liquid Stream

ROBERT L. STEINBERGER and ROBERT E. TREYBAL

New York University, New York 53, New York

Solution rates of ½-, ¾-, and 1-in. cast benzoic acid spheres were measured under natural- and forced-convection conditions. Upward-flowing streams of water and aqueous propylene glycol, in laminar and turbulent flow, were used to contact single spheres in either a 1.50- or 4.00-in.-diameter column. Sphere Reynolds numbers ranged from 10 to 16,920; Schmidt numbers from 987 to 69,680; sphere- to column-diameter ratios, d_S/d_C, from 0.123 to 0.497; and Grashof numbers from 5,130 to 125,200.

The Sherwood number was found independent of the laminar-turbulent transition for pipe flow and the sphere- to column-diameter ratio when the Reynolds number is based on the average fluid velocity and sphere diameter.

A correlation of the data based on the additivity of the natural and forced convection processes is proposed, and statistical analyses of the new experimental data result in equations which correlate other heat and mass transfer data for single spheres immersed in bounded and free-jet streams of gases and liquids for $N_{Re,S}$ from 1 to 30,000 and N_{Sc} from 0.6 to 3,000, within an average deviation of about 20%.

Dimensional analysis has been applied to problems involving the transfer of mass and heat from bodies immersed in fluid streams. In the case of a single sphere the results are

$$N_{Sh} = N_{Sh}(N_{Re}, N_{Sc}, N_{Gr}) \qquad (1)$$

$$N_{Nu} = N_{Nu}(N_{Re}, N_{Pr}, N_{Gr}) \qquad (2)$$

The actual form of the functions are not obtainable by dimensional analysis techniques, and resort must therefore be made to theory or experiment. The terms involved in Equations (1) and (2) are the result of a consideration of radial diffusion and natural and forced convection, the processes by which mass or heat may be transferred from from a sphere.

The first process, by radial diffusion, arises when $N_{Gr} = 0$ and $N_{Re} = 0$. Natural-convective transport arises when $N_{Gr} > 0$, and forced convection occurs when $N_{Re} > 0$. In an actual transport problem the above processes may act singly or in concert, depending upon the flow and diffusional characteristics of the system.

RADIAL DIFFUSION

The process of radial diffusion from a sphere to an infinite stagnant fluid has been treated theoretically by Langmuir (*24*), who shows that

$$N_{Sh,0} = N_{Nu,0} = 2 \qquad (3)$$

Equation (3) has been verified experimentally with drops of relatively low-volatility liquids and solids vaporizing into low-temperature surroundings at near-atmospheric pressures (*14, 25, 26, 38, 42*).

In the case of air streams flowing past evaporating droplets a value of $N_{Sh,0}$ approaching 2 was observed as the Reynolds number was lowered to zero (*5, 33*); however in the case of liquid streams dissolving soluble spheres $N_{Sh,0}$ values from 44 to 100 have been observed which have been attributed to the influence of natural convection (*6, 7*).

NATURAL CONVECTION

Transfer by natural convection is attributed to a current of fluid flowing past a body because of a difference between the bulk and surface fluid densities resulting from concentration differences for the mass transfer problem and because of temperature differences in the case of heat transfer.

An approximate solution of boundary-layer equations is given by Merk and Prins (*29*) for the forward stagnation point of a sphere:

$$N_{Nu,0} = 0.597\,(N_{Gr}N_{Pr})^{1/4} \qquad (4)$$

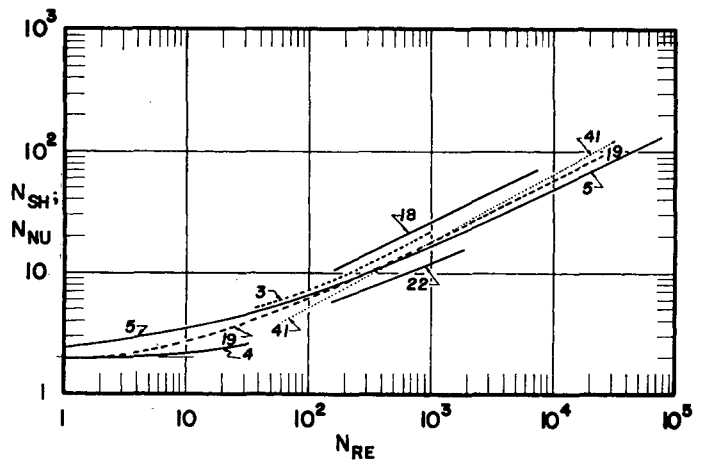

Fig. 1. Transfer from spheres ($N_{Sc} = N_{Pr} = 0.6$).

Robert L. Steinberger is with The Cooper Union, New York, New York.

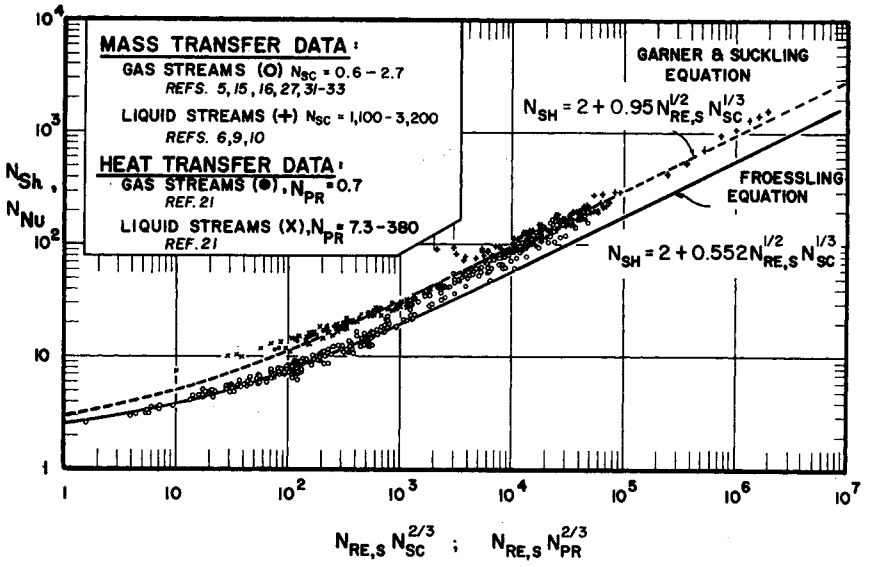

Fig. 2. Mass and heat transfer data for spheres.

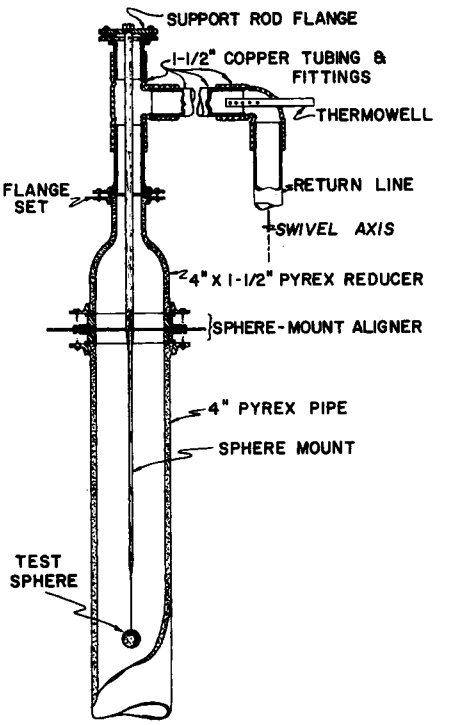

Fig. 3. Details of test section.

which is limited to laminar boundary-layer flow, that is ($N_{Gr}N_{Pr}$) less than 10^8 and N_{Pr} greater than 10. At present no analytical solutions are available for the entire surface of a sphere for either laminar or turbulent boundary-layer flow. Nusselt (*30*) indicates that $N_{Nu,0}$ may be related to ($N_{Gr}N^3_{Pr}$) for fully turbulent boundary-layer flow, but no data are available.

Piret and co-workers (*23, 28*), working with heat and mass transfer from solid spheres to gases, propose

$$N_{Sh,0} = 2 + 0.5\,(N_{Gr}N_{Sc})^{0.25} \quad (5)$$

for ($N_{Gr}N_{Sc}$) from 10^2 to 10^5 and somewhat similar expressions for heat transfer.

FORCED CONVECTION

Several analytical expressions have been developed by considering the hydrodynamics and diffusional characteristics for a sphere. A completely rigorous expression is not yet available. The problem is confounded by the development of flow separation and wake formation on the rear surface of a sphere even for Reynolds numbers, $N_{Re,S}$, as low as 20 (*6*).

Several analytical attempts have been made to characterize transfer rates. Potential-flow theory leads to functions for Equation (1) involving $N_{Pe}^{1/2}$ (*18, 19, 20*), while boundary-layer theory involves $N_{Re}^{1/2}N_{Sc}^{1/3}$ (*5, 7*) or more complex functions (*4*). These relations are summarized in Figure 1 for the special case of $N_{Sc} = N_{Pr} = 0.6$.

Froessling (*5*) measured evaporation rates of spheres into air and correlated his data with a semiempirical equation:

$$N_{Sh} = 2 + 0.552\,N_{Re,M}^{1/2}N_{Sc}^{1/3} \quad (6)$$

Others have correlated similar data by expressions of the same form (*13, 16, 32, 33, 37, 39, 40, 41*). The coefficients recommended range from 0.33 to 1.5 with exponents of the Reynolds number from 0.35 to 0.6. In some cases the radial diffusion term $N_{Sh,0} = 2$ of Equation (6) has been omitted; in others velocities other than the approach velocity have been used. These experiments cover the range of N_{Sc} from 0.6 to 2.7 and $N_{Re,M}$ from 0 to 48,000. Ingebo (*17*), working at temperatures up to 1,000°F., found it necessary to change the form of Equation (6) considerably. An excellent summary of atomization and evaporation of liquid fuels is presented by Graves and Bahr (*12*).

Liquid systems have received little attention. All work has involved the dissolution of benzoic and adipic acid spheres mounted in water streams flowing in either horizontal or vertical pipes. Gates and Shanks (*10*) mounted

Table 1. Cast Sphere Dimensions

Nominal size, in.	Number of spheres measured	Mean of average diameters, in.	Standard deviation from mean, in.
½	36	0.495	0.005
¾	25	0.748	0.003
1	32	0.995	0.005

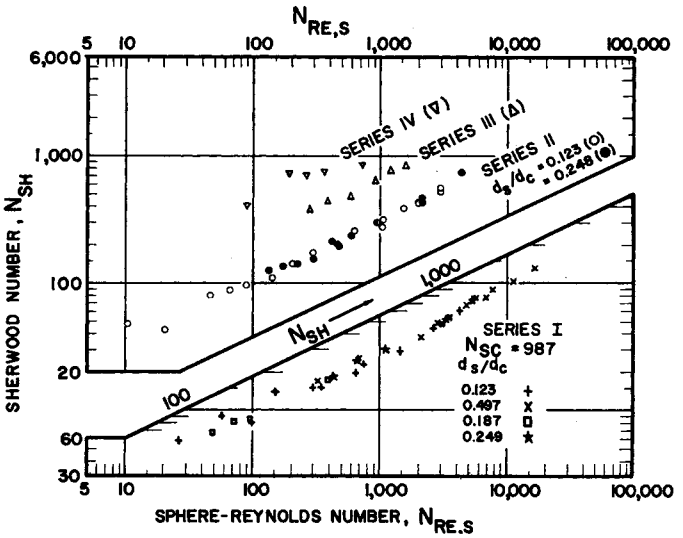

Fig. 4. Experimental data—N_{Sh} vs. $N_{Re,S}$.

Table 2. Ranges of Parameters—Forced-Convection Experiments

Series (N_{Sc})	Subset	d_S/d_C	No. of runs	Reynolds number range $N_{Re,C}$	$N_{Re,S}$	($N_{Gr}N_{Sc}$) $\times 10^{-7}$
	A	0.123	11	218-35,400	26-4,340	1.50
I	B	0.497	11	680-34,000	335-16,920	5.19
(987)	C	0.187	5	264-16,400	49-3,060	5.23
	D	0.249	5	1,820-21,800	450-5,410	12.4
II	A	0.123	18	84-24,640	10-3,000	1.14
(2,220)	B	0.248	11	543-17,770	135-4,400	9.31
III (14,970)		0.185	6	1,510-8,610	280-1,600	12.5
IV (69,680)		0.247	5	371-2,970	92-733	94.5

cast spheres on shafts which were normal to the flow. The range of $N_{Re,S}$ was 1,500 to 11,000, with N_{Sc} approximately 3,000. Garner and Grafton (6) used pressed pellets mounted on the downstream side in a horizontal pipe. Local and over-all mass transfer rates were determined by taking photographs, which necessarily require that a substantial portion of the pellet be dissolved, thereby changing sphericity. Over-all rates were correlated by Garner and Grafton by

$$N_{Sh} = 44 + 0.48\, N_{Re,S}^{1/2} N_{Sc}^{1/3} \quad (7)$$

where the limiting value of 44 was explained on the basis of natural convection.

Garner and Suckling (9), using the same apparatus and techniques and a variety of sphere sizes, gathered additional data and recorrelated the new and old results by replacing the 44 by 2 and the 0.48 by 0.95. Garner and Keey (7), using a vertical pipe, found a difference in rates depending upon the direction of the liquid flow. Results are presented graphically. All of the Garner work is in the range of $N_{Re,S}$ from 2 to 840, N_{Sc} from 788 to 1,680, and laminar flow of the solvent stream.

Kramers (21) measured heat transfer rates from spheres to fluids in laminar flow and correlated the data with a modification of Equation (6) by using an additional N_{Pr} term.

In the case of spheres immersed in liquids flowing through pipes the sphere- to-column-diameter ratio, d_S/d_C, has been varied from 1/8 to 0.3 with no observable wall effect when the sphere–Reynolds number is used.

The data thus far available are exhibited in Figure 2. Two distinct belts of data are seen. The lower region, typified by Froessling's equation (6), contains most of the data for gas systems (N_{Sc} = 0.6 to 2.7). The liquid-system data (N_{Sc} = 1,100 to 3,200), exemplified by the equation of Garner and Suckling, give N_{Sh} values nearly twice those of the gas stream experiments at the same value of $N_{Re,S}N_{Sc}^{2/3}$. No thorough experimental study of the effect of the Schmidt number has been made, and the effect of natural convection remains uncertain.

APPARATUS AND EXPERIMENTAL METHOD

In the present work spheres were cast from benzoic acid. After its dimensions and weight had been measured, a single sphere was mounted in a vertical, cylindrical test section of a flow apparatus. Solvent, flowing upward at constant temperature and flow rate, contacted the sphere for a measured time interval. Upon removing the sphere and reweighing when dry, one could determine the loss in weight.

Sphere Preparation

A length of 2-in.–diameter hot-rolled steel was faced in a lathe to a smooth finish. A round-end mill, mounted in the tailstock, was fed into the face of the rotating stock, thus forming a hemispherical depression. Drilling beyond the radial depth at a slow feed rate gave an extremely smooth finish to the cavity. To form a true hemisphere, face cuts were taken until depth-gauge measurements indicated radial depth of the cavity. The final facing was made to produce a smooth finish. The completed half mold was then cut from the stock. The other half of the mold was produced by repeating the entire procedure. To test for sphericity and to align the two halves, a steel ball bearing was placed in the spherical cavity formed by the molds. Remachining was done when necessary.

A sprue hole and support rod hole were drilled radially between the two clamped parts, the ball bearing serving to align the assembly. A thermocouple hole was

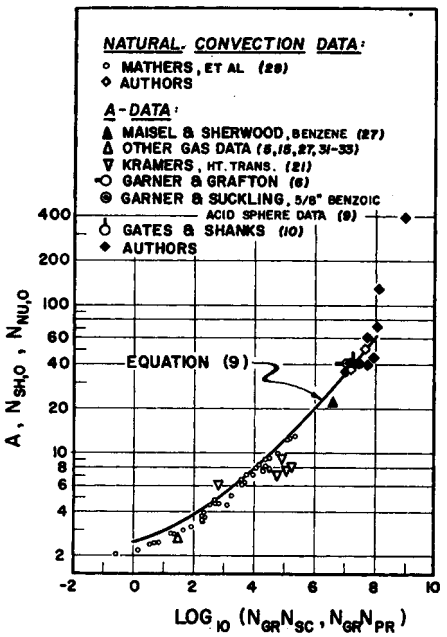

Fig. 5. Plot of $A = N_{Sh,\,o} = N_{Nu,\,o}$ vs. $(N_{Gr}N_{Sc})$, $(N_{Gr}N_{Pr})$.

Table 3. Physical Properties of Solutions

Solubility

Benzoic acid in water (15.0° to 30.0°C.)

$\log_{10}$ (C_S, g./liter; ±0.5%) = 4.2066 to 1,098/T

Benzoic acid in aqueous propylene glycol (15.0° to 25.0°C., W = 40.0 to 60.0 wt. % glycol on an acid-free basis):

$\log_{10}$ (C_S, g./liter; ±1.7%) = 6.898 + 0.0301(W-40) − 1,710/T

Kinematic viscosity

Aqueous propylene glycol solutions (15.0° to 25.0°C., W = 40.0 to 60.0 wt. % glycol on an acid-free basis):

$\log_{10}$ (ν, centistokes; ±1%) = (26.86W + 463.4)/T − (1.6266 + 0.07467W)

Diffusion coefficient at 25.00 ± 0.005°C.

Benzoic acid,

in water:

D = (9.084 ± 0.028)(10^{-6}) sq. cm./sec.

in 40.0 wt. % propylene glycol:

D = (2.336 ± 0.028)(10^{-6}) sq. cm./sec.

in 60.0 wt. % propylene glycol:

D = (1.144 ± 0.032)(10^{-6}) sq. cm./sec.

Density

Benzoic acid-water solutions:

$\log_{10}$ ($\Delta\rho/C\rho_o$) = 305/T − 1.745; ± 10%, max. in Δ_f/ρ_o.

Benzoic acid in 40.0 wt. % propylene glycol, saturated, at 25.00°C.: $\Delta\rho/\rho_o$ = 1.571 × 10^{-3}, ± 2.0%; ρ_o = 1.0293.

Benzoic acid in 60.0 wt. % propylene glycol, saturated, at 25.00°C.: $\Delta\rho/\rho_o$ = 5.052 × 10^{-3}, ± 2.7%; ρ_o = 1.0438.

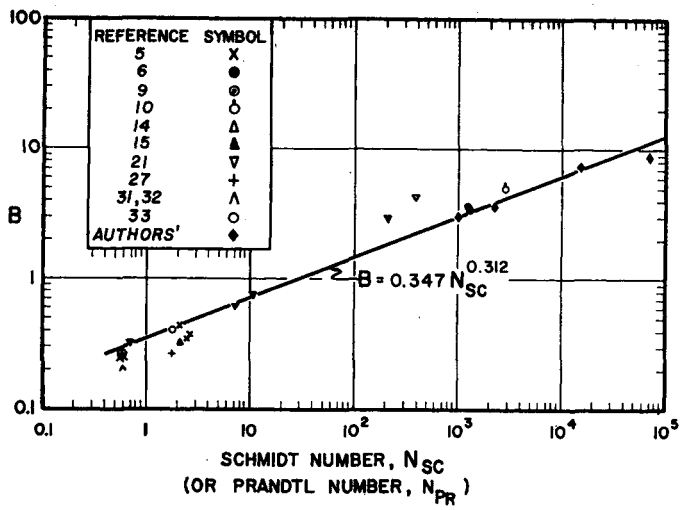

Fig. 6. Plot of B vs. N_{Sc}, N_{Pr}.

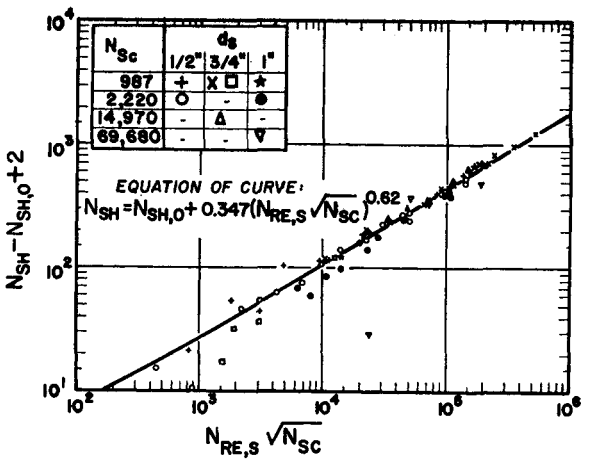

Fig. 7. Correlation of new experimental data.

drilled behind the cavity. Molds for 1/2-, 3/4-, and 1-in. spheres were made.

A 4- to 6-in. length of 304 stainless steel rod 0.043 in. in diameter served as a support rod for each sphere. The rod, with a three-dimensional hook at the end to prevent its removal from the finished casting, was positioned between the mold halves. Spheres were then cast by charging the heated mold with molten benzoic acid. The cast spheres were inspected, excess sprue material was removed with a file, and the spheres were polished with a wad of absorbent cotton. The specimens thus obtained were shiny, white, nearly perfect spheres. Six micrometer measurements of diameter, to the nearest 0.0005 in., were taken at intervals on the equator. An average deviation of 0.002 in. from the mean was obtained for any one sphere. Table 1 shows the dimensions of the cast spheres prior to use in the mass transfer studies. The spheres were suspended in individual stoppered flasks containing Drierite by implanting their support rods into the face of the rubber stoppers.

Flow Apparatus

Fluid was circulated from a tank, through a heat exchanger and flow meters, and into the bottom of a test column, whence the solvent was returned to the tank. Pulsations were damped by a surge tank. The test columns were 15-ft. lengths of 1.50- and 4.00-in. I.D. Pyrex glass pipes. Inlet and exit temperatures at the test section were measured to indicate heat effects from the laboratory; the exit temperature, taken as that at the sphere, was measured to within 0.1°C.

Figure 3 shows the details of the method of mounting the test spheres in the 4-in. column. The swivel-pipe arrangement permitted connection to the 1.50-in. column. The tapered specimen mount had an over-all length of 32 in. and was composed of a 1/2-in. shaft axially connected to a 1/4-in. shaft. A 0.043-in.–diameter hole drilled into the end of the 1/4-in. shaft permitted the insertion of the test sphere support rod. A flange with slotted screw holes was bolted to the 1/2-in. shaft. The mount was streamlined by turning a 5 deg. nose cone at one end of each shaft prior to assembly. The transitions were smoothed and polished with fine emery paper.

To align the sphere and mount at the center of the column and to provide stability during a run, another contact point was made. A 1.50-in. high, 4.00-in. I.D. by 5-in. O.D. Dural ring was flanged between the column and reducer. Three 1/4- by 5-in. brass slide rods in compression fittings, mounted 120 deg. apart in the midplane of the ring, centered the mount in the column. A similar tripod affair was made for the 1.50-in. column.

The above practices provided a stable, coaxial mounting for the test spheres. Disturbances in the flow pattern around the sphere were minor because the mount was streamlined and present on the downstream side of the test specimen. The sphere was located approximately 16 in. from the top of the cylindrical section, thus making a 13-2/3-ft.-long calming section available to the flowing solvent.

Procedure

Solvents used were water and aqueous propylene glycol solutions. The solvent level in the test column was lowered below the sphere position. A sphere, weighed to the nearest 0.05 mg. and measured to the nearest 0.0005 in., was mounted and the solvent circulation started. A stop watch was started when the rising solvent contacted the sphere. At the end of the test the site was drained rapidly and the sphere was removed and placed in its flask to dry. In the case of the glycol runs the spheres were vacuum washed five times with distilled water to remove the glycol. The washings were titrated for benzoic acid and the sphere was dried as for the water runs. The spheres were weighed during their drying periods.

Final sphere weights were not obtainable as such since the tested spheres never reached a final weight on drying. Sublimation of benzoic acid from the surface of the spheres took place continuously. Weight losses were plotted against time, and the resulting straight lines were extended to zero drying time to give the extrapolated weight losses due to solution.

The following represent the changes in the indicated quantities encountered in the forced convection experiments:

Sphere diameter:	0.012 in., maximum
Run temperature:	± 0.2°C., maximum
Flow rate:	± 1% for water runs,
	± 2% for glycol runs

Average extrapolated weight losses were 58 mg. for the 1/2-in., 90 mg. for the 3/4-in., and 169 mg. for the 1-in. spheres. These weight changes are from 1.6 to 3% of the initial sphere weights and yield calculated diameter reductions of 0.5 to 1.6%. The ranges of operating conditions for the forced convection experiments are listed in Table 2.

Other Tests

The velocity distribution for water flowing in the 4.00-in. conduit was determined by pitot-static tube traverses. The velocity data indicate a distribution symmetrical about the column center line and agreed with the Nikuradse generalized velocity distribution (*34*) with a mean deviation of about 2%.

Two natural-convection experiments were performed. A 1 qt. Dewar flask was filled with water and allowed to stand for 8 hr. on a 1/4-in.–thick rubber pad to damp fluid circulations. A benzoic acid sphere was gently lowered into the stagnant fluid, a Lucite cover being used to support the sphere and a thermometer. The next day the sphere was gently removed from the flask, and the solution was mixed and titrated for its benzoic acid content.

The necessary physical properties of the benzoic acid solutions were measured, and the results are listed in Table 3. In the case of the diffusion coefficient the procedure of Gilliland, Baddour, and Goldstein (*11*) was used.

RESULTS

A summary of the computed results is given in Table 4*; detailed data appear elsewhere (*36*).

* Tabular material has been deposited as document 6264 with the American Documentation Institute, Photoduplication Service, Library of Congress, Washington 25, D. C., and may be obtained for $1.25 for photoprints or $1.25 for 35-mm microfilm.

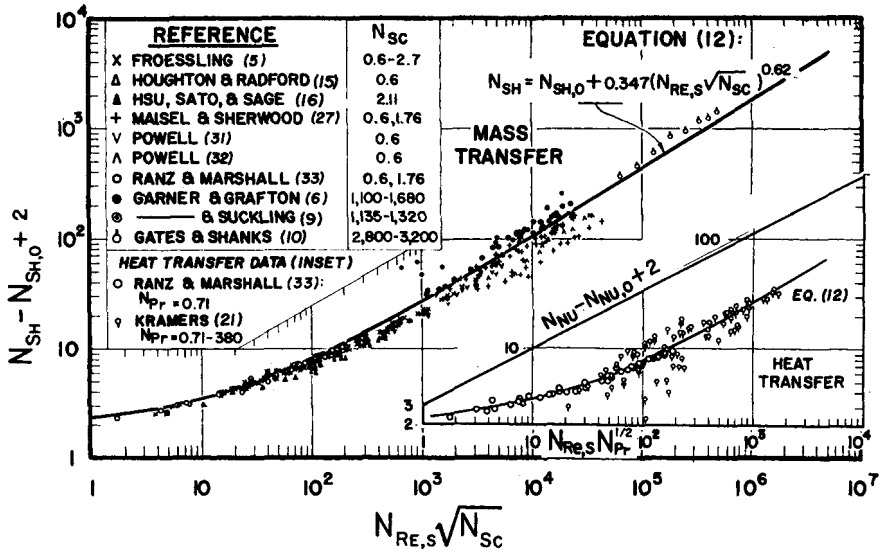

Fig. 8. Comparison of correlation equations with literature data.

Effect of Reynolds Number

The experimental data were first tested for dependence on flow rate by assuming the average fluid velocity in the pipe to be the correlating parameter. A plot of N_{Sh} vs. $N_{Re,c}$ showed no effect of the laminar to turbulent transition for pipe flow. The data when plotted in this way showed a marked dependence on the ratio of the sphere-to-pipe diameter. This dependence disappeared, as shown in Figure 4, when the sphere-Reynolds number was used, and as a result subsequent correlations are based upon this. Reynolds numbers other than $N_{Re,s}$, based on d_s, were tried for correlating N_{Sh} with N_{Re}. When the fluid velocity at the sphere axis (approach velocity), the average velocity intercepted by the projected sphere area, or the average velocity in the minimum flow area between the sphere and the column wall were used to calculate Reynolds numbers, the resulting N_{Sh} vs. N_{Re} plots showed distinct separation according to d_s/d_c.

Proposed Correlation

It was possible to correlate the data by an expression of the form

$$N_{Sh} = A + B(N_{Re,s})^n \qquad (8)$$

The proposed-correlation equation predicts a value of $N_{Sh,0} = A$ when $N_{Re,s} = 0$. This limiting case is significant since mass transport occurs by natural convection when $N_{Re} = 0$. The quantity A accounts for the curvature of the data plotted in Figure 4 and is taken to be a function of the Grashof and Schmidt moduli. At high $N_{Re,s}$ the forced-convection process predominates over the natural convection process, and N_{Sh} becomes nearly equal to $B(N_{Re,s})^n$. The quantity B accounts for the majority of the displacement between the data of series I, II, III, and IV at high $N_{Re,s}$ and is taken to be a function of N_{Sc}. Equation (8) thus proposes the additivity of the natural- and forced-convective processes. Other interpretations of the natural- forced-convective phenomena are also possible as indicated by the recent theoretical paper of Acrivos (*1*). To extract the best value of A, B, and n from the experimental data, statistical analyses of the data were performed.

The forced-convection data of series I and II were applied to Equation (8), and statistical analyses of the data were performed. Since Equation (8) contains three unknowns, A, B, and n, and two knowns, values of n were assumed. The data for the various sphere sizes were pooled, and the criterion of least variance of the pooled estimate was used to find the best value of n.

With n taken as 0.5 or 0.7 the data should not be pooled with less than a 1% chance of being in error. For intermediate values of n the variance of the pooled estimate passed through a minimum at $n = 0.62$, and this value was therefore taken for further correlation. Correlation coefficients greater than 0.993 were obtained for the experimental data of series I, II, and III, indicating better than 99.9% confidence in Equation (8). A correlation coefficient of 0.811 for series IV indicated a 90 to 95% confidence in the equation. Values of A and B were then computed from the data with n taken as 0.62.

Least-square analyses were performed on the A data and $N_{Sh,0}$ data by weighting the values of A and $N_{Sh,0}$ according to the reciprocal of their variances to obtain A as a function of N_{Gr} and N_{Sc}. It was found necessary to separate the data according to whether $(N_{Gr}N_{Sc})$ was less than or greater than 10^8, probably because of the onset of a turbulent boundary layer in the higher range (8). For $(N_{Gr}N_{Sc})$ less than 10^8

$$A = N_{Sh,0} = 2 + 0.569(N_{Gr}N_{Sc})^{(0.250)_2} \qquad (9)$$

with an average deviation of the data of 12.7%, and for $(N_{Gr}N_{Sc})$ greater than 10^8

$$A = N_{Sh,0} = 2 + 0.0254(N_{Gr}N_{Sc})^{1/3}(N_{Sc})^{0.244} \qquad (10)$$

with an average deviation of 3.2%. The three points of series ID, III, and IV are the only data available for establishing Equation (10). In the case of Equation (9) a comparison of the equation, the new experimental data, and natural-convection mass transfer data (*28*) is shown in Figure 5. Also included are A values obtained from plots of N_{Sh} (or N_{Nu}) vs. $N_{Re,s}^{0.62}$ with data used from the literature (*5, 15, 16, 27, 31, 32, 33, 6, 9, 10, 21*). The agreement is excellent.

Weighted least-square analyses were performed on the B data with the result that

$$B = 0.347\,N_{Sc}^{0.812} \qquad (11)$$

with an average deviation of 1.80%. It is interesting to note that the Colburn (2) exponent of 1/3 on the Schmidt number is included within one standard deviation (±0.0204) of 0.312. The new B values, together with those determined from plots of N_{Sh} (or N_{Nu}) vs. $N_{Re,s}^{0.62}$ with data used from the literature, are compared with Equation (11) in Figure 6. Again the agreement is excellent.

The final correlation is

$$N_{Sh} = N_{Sh,0} + 0.347(N_{Re,s}N_{Sc}^{1/2})^{0.62} \qquad (12)$$

with $N_{Sh,0}$ defined by Equations (9) and (10).

For purposes of graphical comparison of the experimental data and the correlation equations a logarithmic plot of $(N_{Sh} - N_{Sh,0} + 2)$ vs. $(N_{Re,s}N_{Sc}^{1/2})$ is proposed. This procedure reduces the experimental data to a natural-convection-free basis.

Equations (9) and (10) and the values of N_{Gr} and N_{Sc} were used to calculate values of $(N_{Sh,0} - 2)$. These values were then subtracted from the experimental values of N_{Sh} and the results plotted against $(N_{Re,s}N_{Sc}^{1/2})$ in Figure 7. The solid line is that of Equation (12). The data show excellent agreement with the final correlating equations. Errors in the low end of the scale are exaggerated because of the subtraction of $N_{Sh,0}$ from N_{Sh}.

Figure 8 is a plot of the experimental data from the literature computed in accordance with the relations proposed here. The ability of Equations (9) and (12) to correlate both gas- and liquid-stream data and heat as well as mass transfer data is most important; previous correlations, experimental and theoretical, are not capable of doing this.

It is interesting that the above equations, developed from the new data which range from 841 $<(N_{Re,s}N_{Sc}^{1/2})$ <531,000, correlate other data ranging from 1 $<(N_{Re,s}N_{Sc}^{1/2})$<500,000. The low range is handled exceptionally well by the new equations with about a 3% average deviation. The new data of Garner and Keey (7) for $N_{Re,s}$ from 1 to 20, N_{Sc} = 788, represent an exception to this. In the higher ranges the literature data scatter evenly above and below the curve of Figure 8 with an average deviation of about 20%.

Since the work reported here was completed, some additional data have appeared (35). The presently proposed equations correlate these data reasonably well, but distinct deviations due, it is felt, to inadequate diffusivities nevertheless remain.

ACKNOWLEDGMENT

The authors are grateful to the National Science Foundation for its support under Grant G-598. This paper is a condensation of a thesis submitted by Robert L. Steinberger in partial fulfillment of the requirements for the degree of Doctor of Engineering Science at New York University.

NOTATION

A = value of N_{Sh} extrapolated to N_{Re} = 0, dimensionless
B = coefficient, dimensionless
C = concentration of solute in solution, g./cc.
C_s = saturation concentration, g./liter
D = diffusion coefficient, sq. cm./sec.
d_c = column or pipe diameter, cm.
d_s = sphere diameter, cm.
g = local acceleration due to gravity, cm./sec.^{2}
h = heat transfer coefficient, cal./(sq. cm.)(sec.)(°C.)
K = mass transfer coefficient, cm./sec.
k = thermal conductivity, cal./(cm.)(sec.)(°C.)
L = characteristic dimension of system, cm.
N_{Gr} = Grashof number, $gd_s^3(\rho_s-\rho_o)/(\rho_o\nu^2)$; dimensionless
N_{Nu} = Nusselt number, hL/k, dimensionless
$N_{Nu,0}$ = value of N_{Nu} at N_{Re} = 0, dimensionless
N_{Pe} = Peclet number, equal to $(N_{Re}N_{Sc})$ or $(N_{Re}N_{Pr})$, dimensionless
N_{Pr} = Prandtl number, ν/α, dimensionless
N_{Re} = Reynolds number, LV/ν, dimensionless
$N_{Re,C}$ = column Reynolds number, d_cU/ν, dimensionless
$N_{Re,M}$ = Reynolds number based on approach velocity at sphere axis, d_sU_M/ν, dimensionless
$N_{Re,S}$ = sphere Reynolds number, d_sU/ν, dimensionless
N_{Sc} = Schmidt number, ν/D, dimensionless
N_{Sh} = Sherwood number, Kd_s/D, dimensionless
$N_{Sh,0}$ = value of N_{Sh} at N_{Re} = 0, dimensionless
n = exponent of $N_{Re,S}$, dimensionless
T = absolute temperature, °K.
U = average fluid velocity, cm./sec.
U_M = approach velocity at axis of sphere, cm./sec.
V = characteristic velocity of system, cm./sec.
W = wt. % propylene glycol in water solutions, on a benzoic acid–free basis

Greek Letters

α = thermal diffusivity, sq. cm./sec.
ν = kinematic viscosity, sq. cm./sec.
ρ_o = solvent density, g./cc.
ρ_s = solution density, g./cc.
$\Delta\rho$ = solution minus solvent density $\rho_s-\rho_o$, g./cc.

LITERATURE CITED

1. Acrivos, Andreas, *A.I.Ch.E. Journal*, 4, 285 (1958).
2. Colburn, A. P., *Trans. Amer. Inst. Chem. Engrs.*, 29, 174 (1933).
3. Drake, R. M., P. M. Sauer, and S. A. Shaaf, *Inst. Eng. Res. Rept. He-150-74*, Univ. Calif., Berkeley (Nov. 15, 1950).
4. Friedlander, S. K., *A.I.Ch.E. Journal*, 3, 43, (1957).
5. Froessling, Nils, *Gerland's Beit. zur Geophys.*, 52, 170 (1938).
6. Garner, F. H., and R. W. Grafton, *Proc. Roy. Soc. (London)*, A224, 64 (1954).
7. Garner, F. H., and R. B. Keey, *Chem. Eng. Sci.*, 9, 119 (1958).
8. *Ibid.*, 9, 218 (1959).
9. Garner, F. H., and R. D. Suckling, *A.I.Ch.E. Journal*, 4, 114 (1958).
10. Gates, R. P., and R. Shanks, S. M. thesis, Mass. Inst. Technol., Cambridge (1949).
11. Gilliland, E. R., R. F. Baddour, and D. J. Goldstein, *Can. J. Chem. Eng.*, 35, 10 (1957).
12. Graves, C. C., and D. W. Bahr, *Natl. Advisory Comm. Aeronaut. Rept. 1300*, 1-31 (1957).
13. Gröber, H., S. Erk, and U. Grigull, "Grundgesetze der Wärmeübertragung," Springer-Verlag, Berlin, Germany (1957).
14. Houghton, H. G., *Physics*, 4, 419 (1933).
15. ———, and W. H. Radford, *Papers Phys. Oceanog. Meteorol., Mass. Inst. Tech. and Woods Hole Oceanog. Inst.*, 6, No. 3 (1938).
16. Hsu, N. T., K. Sato, and B. H. Sage, *Ind. Eng. Chem.*, 46, 870 (1954).
17. Ingebo, R. D., *Chem. Eng. Progr.*, 48, 403 (1952).
18. Johnstone, H. F., and R. V. Kleinschmidt, *Trans. Am. Inst. Chem. Engrs.*, 34, 181 (1938).
19. Johnstone, H. F., R. L. Pigford, and J. H. Chapin, *Eng. Exp. Sta. Bull. 330*, Univ. Ill., Urbana (June 17, 1941).
20. Johnstone, H. F., and G. C. Williams, *Ind. Eng. Chem.*, 31, 993 (1939).
21. Kramers, H. A., *Physica*, 12, 61 (1946).
22. Kudryashev, L. I., *Transl. No. 368, British R.A.E.* (March, 1951).
23. Kyte, J. R., A. J. Madden, and E. L. Piret, *Chem. Eng. Progr.*, 49, 653 (1953).
24. Langmuir, Irving, *Phys. Rev.*, 12, 368 (1918).
25. Langstroth, G. O., C. H. Diehl, and E. J. Winhold, *Can. J. Research*, 28A, 580 (1950).
26. Luchak, G., and G. O. Langstroth, *ibid.*, 574 (1950).
27. Maisel, D. S., and T. K. Sherwood, *Chem. Eng. Progr.*, 46, 131 (1950).
28. Mathers, W. G., A. J. Madden, and E. L. Piret, *Ind. Eng. Chem.*, 49, 961 (1957).
29. Merk, H. J., and J. A. Prins, *Appl. Sci. Res.*, A4, 11, 195 (1954).
30. Nusselt, W., *Gesundheits Ing.*, 38, 477 (1915).
31. Powell, R. W., *Proc. Brit. Assoc. Refrig.*, 36, 61 (1939-40).
32. ———, *Trans. Inst. Chem. Engrs. (London)*, 18, 36 (1940).
33. Ranz, W. E., and W. R. Marshall, Jr., *Chem. Eng. Progr.*, 48, 141, 173 (1952).
34. Schlichting, Hermann, "Boundary-Layer Theory," McGraw-Hill, New York (1955).
35. Steele, L. R., and C. J. Geankoplis, *A.I.Ch.E. Journal*, 5, 178 (1959).
36. Steinberger, R. L., D. Eng. Sci. thesis, New York Univ., New York (1959).
37. Tang, Y. S., J. M. Duncan, and H. E. Schweyer, *Natl. Advisory Comm. Aeronaut. Tech. Note 2867* (1953).
38. Topley, B., and R. W. Whytlaw-Gray, *Phil. Mag.*, 4, 873 (1927).
39. Tverskaya, N. P., *Izvest. Akad. Nauk. SSSR. Ser. Geog. Geofiz.*, 14, 164 (1950).
40. van Krevelen, D. W., and P. J. Hoftijzer, *J. Sci. Chem. Ind.*, 68, 59 (1949).
41. Williams, G. C., Sc. D. thesis, Mass. Inst. Technol., Cambridge (1942).
42. Woodland, D. J., and E. Mack, Jr., *J. Am. Chem. Soc.*, 55, 3149 (1933).

Manuscript received June 26, 1959; revision received October 9, 1959; paper accepted October 12, 1959. Paper presented at A.I.Ch.E. San Francisco meeting.